*Journal of Sound and Vibration* (2000) **229**(5), 1097–1113
doi:10.1006/jsvi.1999.2597, available online at http://www.idealibrary.com on IDEAL®

# PARAMETRIC INSTABILITY OF A LEIPHOLZ COLUMN UNDER PERIODIC EXCITATION

B. KANG AND C. A. TAN

*Department of Mechanical Engineering, Wayne State University, Detroit, MI* 48202, *U.S.A.*

(*Received* 25 *March* 1999, *and in final form* 21 *July* 1999)

In this paper, the parametric instability of a Leipholz column under four boundary conditions is examined. The study of this prototypical model is intended to provide a basic understanding of the disc brake pad instability. The distributed, follower-type axial load is assumed to be uniform and periodic. Instability regions are obtained and the existence of combination resonances of the sum and difference types is discussed for each set of boundary conditions. It is found that the combination resonance of the sum type exists in all the cases of boundary conditions considered, but the difference type exists only in the cases of clamped-simply supported and clamped-free boundary conditions. The combination resonance is shown to be as important as the simple parametric resonance. Results, when compared to a column under a periodic end load, show that the instability characteristics of these two columns are considerably different. The effect of a constant axial load is to shift the instability regions along the frequency axis.



## 1. INTRODUCTION

When an elastic beam is subjected to an axial compressive load, there exist critical loads at which the beam buckles or flutters depending on the boundary conditions and the application of the load. Beck [1] was the first to solve the flutter instability of a cantilever beam under a tangential, compressive end load. This type of load is called a follower-force which renders the system non-conservative, and the stability of the system must in general be solved by a dynamic approach. Extensive studies on the buckling and flutter of beams are well documented [2–6].

Among the follower-force problems, Leipholz [7, 8] examined the stability of a beam subjected to an uniformly distributed axial load, called the *Leipholz column*, under four sets of boundary conditions: pinned–pinned, clamped–clamped, clamped–pinned, and clamped–free. It was shown that the lowest critical load of the column with one of the first three sets of boundary conditions can be determined by principles of stationarity, though the problems are non-self-adjoint. However, the critical load for the clamped–free Leipholz column is of the flutter type and must be evaluated by means of dynamics.

Parametric instability of columns excited by periodic end loads has been studied extensively [3, 9, 10]. Depending on the boundary conditions, a parametrically

0022-460X/00/051097 + 17 $35.00/0 

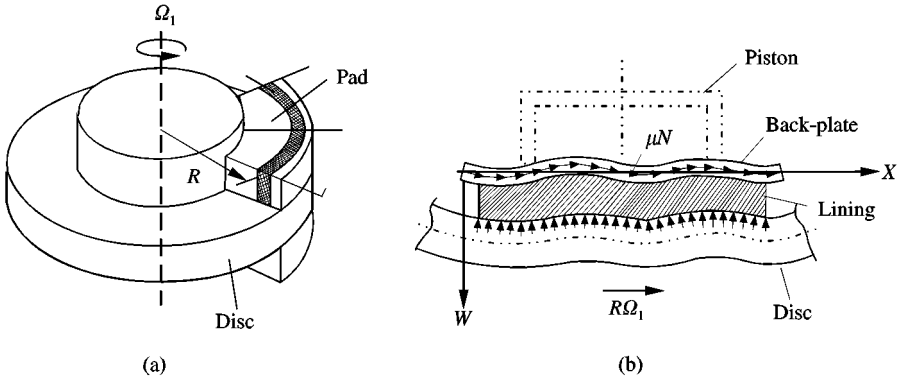


Figure 1. Schematics of a brake disc and pad system: (a) considering a strip of the brake pad, (b) depicting the beam model for the brake disc–pad system.

excited column can exhibit combination resonance of the sum and/or difference types in addition to a simple parametric resonance [9]. This is explained by examining the coupling dynamics of the normal modes of the unloaded problem [11]. For example, combination resonance does not occur for a simply supported column since inter-modal coupling does not exist. Parametrically excited systems are time-dependent and closed-form solutions generally do not exist. Approximate methods such as perturbations [11], harmonic/spectral balance method [12, 13], incremental harmonic balance method [14] and Chebyshev-polynomial-based numerical procedure [15] have been applied.

The purpose of this paper is to study the stability of a Leipholz column under periodic loads. In particular, the effects of various boundary conditions on the system stability are examined. The motivation of this work comes from a recent study on the instability of disc brakes [16]. The necessary background for the equation of motion is described in Appendix A. Consider a rotor (disc) and pad system commonly employed in automotive and aircraft brakes, as shown in Figure 1(a). Experimental results have shown that there is no nodal circle in the disc vibration during brake squeal [17, 18], and that the pad and its boundary conditions† contribute significantly to the generation of brake noise [17–19]. For these reasons, the dynamic stability of a strip of the pad, modelled as a beam (depicted in Figure 1(b)), is investigated. Here, the frictional traction $\mu N$ ($N$ is the normal contact force) is a distributed follower-type force tangential to the beam. It is shown in Appendix A that the frictional traction depends on the disc rotating frequency $\Omega_1$, the disc vibration frequency $\Omega_2$, and other parameters. Since $\Omega_2 \gg \Omega_1$ and $\Omega_1 \ll 1$ for most brake applications, the effects of $\Omega_1$ are neglected as a first approximation and the resulting stability problem becomes fundamentally similar to a Leipholz column under periodic axial loads. To date, the parametric instability of the Leipholz column has not been reported in the literature.

†Felske *et al.* [17] concluded from experiments that there are free–free bending or fastened–free bending motions of the pads. However, it is in general difficult to determine the exact boundary conditions.

This paper is organized as follows. The problem formulation and equation of motion are described in section 2. The response solution based on a Galerkin approach and stability analysis are outlined in section 3. In section 4, numerical results for the parametric stability of the Leipholz column are presented for four basic boundary conditions and are compared to those for the beam under a periodic end load [9].

## 2. PROBLEM FORMULATION

Consider a beam subjected to a distributed axial load which varies periodically with time $T$ as shown in Figure 2(a). Neglecting the coupling between the transverse and axial vibrations, and applying the Euler–Bernoulli beam theory, the equation of motion governing the tranverse vibration $W(X, T)$ of the undamped beam can be expressed as

$$\rho A \frac{\partial^2 W}{\partial T^2} + EI \frac{\partial^4 W}{\partial X^4} + \left( \int_X^L (p_0(\xi) + p(\xi) \cos \Omega T) \, \mathrm{d}\xi \right) \frac{\partial^2 W}{\partial X^2} = 0, \quad X \in (0, L), \, T > 0, \tag{1}$$

where $\rho A$ denotes the mass per unit length of the beam, $EI$ the flexural rigidity, $L$ the span length, $p_0$ and $p$ the static and dynamic load per unit length, respectively, and $\Omega$ the excitation frequency. In this study, $p_0$ and $p$ are assumed to be uniform. Equation (1) is the form of the Leipholz column model [5] and the distributed axial load represents a non-conservative follower-type force directed along the beam's deflection curve. The derivation of equation (1) from a model for the disc brake pad vibration is shown in Appendix A.

Introducing the following non-dimensional variables and parameters,

$$x = \frac{X}{L}, \quad t = \sqrt{\frac{EI}{\rho A}} \frac{T}{L^2}, \quad w = \frac{W}{L}, \quad \hat{p}_0 = \frac{p_0 L^3}{EI}, \quad \hat{p} = \frac{pL^3}{EI}, \quad \omega = \sqrt{\frac{\rho A}{EI}} L^2 \Omega, \tag{2}$$

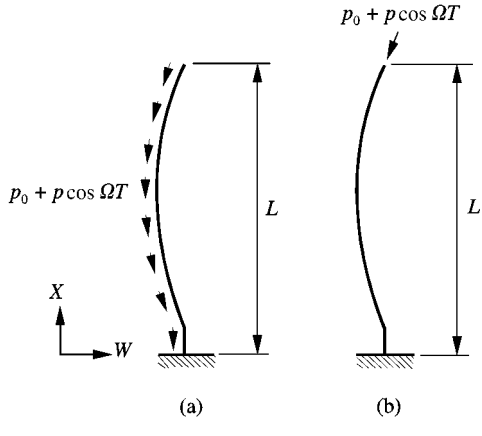


Figure 2. Schematics of a column subjected to (a) a distributed periodic load, (b) a periodic end load.

equation (1) can be expressed as

$$\frac{\partial^2 w}{\partial t^2} + \frac{\partial^4 w}{\partial x^4} + (1 - x)(\hat{p}_0 + \hat{p}\cos\omega t)\frac{\partial^2 w}{\partial x^2} = 0, \quad x \in (0, 1), \quad t > 0. \tag{3}$$

Due to the time dependency of the problem, it is not feasible to obtain a closed-form solution to equation (3). Hence an approximate solution of the following form is sought:

$$w(x, t) = \sum_{m=1}^{N} q_m(t)\varphi_m(x), \tag{4}$$

where $q_m(t)$ is the generalized co-ordinate and $\varphi_m(x)$ is the eigenfunction of the associated unloaded problem of the beam. In this study, four sets of most common boundary conditions are considered, namely simply–simply supported (S–S) or hinged–hinged, clamped–clamped (C–C), clamped–simple (C–S), and clamped-free (C–F). Substitution of $w(x, t)$ from equation (4) into equation (3) and applying the Galerkin's method yields

$$\sum_{m=1}^{N} \left\{ \ddot{q}_m \int_0^1 \varphi_m\varphi_n \,\mathrm{d}x + \lambda_m^4 q_m \int_0^1 \varphi_m\varphi_n \,\mathrm{d}x + (\hat{p}_0 + \hat{p}\cos\omega t) q_m \int_0^1 (1 - x)\varphi_m''\varphi_n \,\mathrm{d}x \right\} = 0,$$

$$n = 1, 2, \ldots, N, \tag{5}$$

where dot $= \partial/\partial t$, $(\,)' = \partial/\partial x$, $\lambda_m^4 = \omega_m^2$, and $\omega_m$ is the non-dimensional $m$th natural frequency of the unloaded beam with specified boundary conditions. The orthonormalization properties of the eigenfunctions are

$$\int_0^1 \varphi_m\varphi_n \,\mathrm{d}x = \frac{\delta_{mn}}{a}, \tag{6}$$

where $\delta_{mn}$ is Kronecker's delta and $a$ is a normalization factor which takes the value of 1 or 2 depending on the boundary conditions. Hence, equation (5) can be rewritten as

$$\ddot{\mathbf{q}} + (\mathbf{A} + a\hat{p}_0\mathbf{B} + a\hat{p}\cos\omega t\mathbf{B})\mathbf{q} = \mathbf{0}, \tag{7}$$

where

$$\mathbf{q} = \{q_1, q_2, \ldots, q_{N-1}, q_N\}^{\mathrm{T}}, \quad \mathbf{A}_{mn} = \lambda_n^4\delta_{nm}, \quad \text{and} \quad \mathbf{B}_{nm} = \int_0^1 (1 - x)\varphi_m''\varphi_n \,\mathrm{d}x,$$

$$m, n = 1, 2, \ldots, N. \tag{8}$$

Equation (7) is a set of $N$ second order, linearly coupled differential equations with periodic coefficients of Hill's type. Note that, due to the non-conservative loading, $\mathbf{B}$ is asymmetric for all of the boundary conditions considered in this paper. However, for columns under periodic end loads, $\mathbf{B}$ is diagonal for the S–S case and is symmetric except for the C–F case [9]. Leipholz [7, 8] referred to three sets of boundary conditions as *fully supported* rods (beams) and classified the critical loads as *divergence* type (S–S case) and *pseudo-divergence* type (C–C and C–S cases) according to the loci of their eigenvalues. It was shown that their lowest critical loads can be determined by means of statics although the problems are non-self-adjoint. Hence, variational principles are applicable to these non-conservative problems.

In what follows, the parametric instability of the Leipholz column represented by the set of coupled Mathieu equations (7) is investigated. To understand the effects of the distributed load on the system stability, results are also compared to those for a column excited by a periodic end load as shown in Figure 2(b).

## 3. STABILITY ANALYSIS

The steady state solution to equation (7) can be approximated by the Fourier series

$$\mathbf{q} \cong \mathrm{e}^{st}\left\{\frac{\mathbf{b}_0}{2} + \sum_{k=1}^{K}(\mathbf{a}_k \sin k\omega t + \mathbf{b}_k \cos k\omega t)\right\}, \tag{9}$$

where $\mathbf{b}_0$, $\mathbf{a}_k$, and $\mathbf{b}_k$ are constant vectors which in general are complex-valued and $s$ is a characteristic exponent. Substituting $\mathbf{q}$ into equation (7) and balancing the harmonic terms, the following system of homogeneous algebraic equations are obtained:

$$\mathbf{a}_0 = \mathbf{0}, \quad (\mathbf{A} + a\hat{p}_0\mathbf{B} + s^2\mathbf{I})\mathbf{b}_0 + a\hat{p}\mathbf{B}\mathbf{b}_1 = \mathbf{0}, \tag{10a, b}$$

$$a\hat{p}\mathbf{B}\mathbf{a}_{k-1} + 2\{\mathbf{A} + a\hat{p}_0\mathbf{B} + (s^2 - k^2\omega^2)\mathbf{I}\}\mathbf{a}_k + a\hat{p}\mathbf{B}\mathbf{a}_{k+1} - 4sk\omega\mathbf{b}_k = \mathbf{0}, \; k = 1, \ldots, K, \tag{10c}$$

$$a\hat{p}\mathbf{B}\mathbf{b}_{k-1} + 2\{\mathbf{A} + a\hat{p}_0\mathbf{B} + (s^2 - k^2\omega^2)\mathbf{I}\}\mathbf{b}_k + a\hat{p}\mathbf{B}\mathbf{b}_{k+1} + 4sk\omega\mathbf{a}_k = \mathbf{0}, \; k = 1, \ldots, K, \tag{10d}$$

where $\mathbf{I}$ denotes the identity matrix. Let $\mathbf{x} = \{\mathbf{b}_0, \mathbf{b}_1, \mathbf{b}_2, \ldots, \mathbf{b}_K, \mathbf{a}_1, \mathbf{a}_2, \ldots, \mathbf{a}_K\}^{\mathrm{T}}$. Equations (10) can then be rearranged into the following form:

$$(\mathbf{M}_0 + s\mathbf{M}_1 + s^2\mathbf{M}_2)\mathbf{x} = \mathbf{0}, \tag{11}$$

where $\mathbf{M}_0$, $\mathbf{M}_1$, and $\mathbf{M}_2$ are the coefficient matrices of ascending powers of $s$. Since $\mathbf{M}_2$ is non-singular, equation (11) is transformed into a state-space form by introducing a state vector $\mathbf{y} = s\dot{\mathbf{x}}$,

$$\begin{bmatrix} \mathbf{0} & \mathbf{I} \\ -\mathbf{M}_2^{-1}\mathbf{M}_0 & -\mathbf{M}_2^{-1}\mathbf{M}_1 \end{bmatrix} \begin{Bmatrix} \mathbf{x} \\ \mathbf{y} \end{Bmatrix} = s \begin{Bmatrix} \mathbf{x} \\ \mathbf{y} \end{Bmatrix}. \tag{12}$$

Note that similar solution methodologies have been applied to study the parametric instability of time-dependent systems [3, 20, 21]. Equation (12) represents an eigenvalue problem with a real asymmetric matrix, and the eigenvalues are complex, $s = s_{real} + \mathrm{i}s_{imag}$, where $\mathrm{i} = \sqrt{-1}$. The sign and magnitude of $s_{real}$ determine the dynamic stability and the amplitude growth rate for the given system, i.e., the steady state response is unbounded (unstable) when $s_{real} > 0$, is oscillatory but bounded (critical case) when $s_{real} = 0$, and is asymptotically stable when $s_{real} < 0$. However, due to unavoidable roundoffs in the numerical computations and practical realization of the unbounded response, the instability boundary is relaxed and chosen to be $s_{real} > 10^{-5}$. The size of the square matrix in equation (12) is $2N(2K + 1)$. In the following numerical studies, $N = 4$ and $K = 10$ are chosen to capture any possible combination resonance and to achieve a satisfactory convergence of the numerical solution in the case of large excitation amplitudes.

## 4. NUMERICAL RESULTS

For the results presented herein, the excitation amplitude and frequency are normalized by a critical buckling/flutter load, $\varepsilon = \hat{p}/\hat{p}_{cr}$, and the first natural frequency of the unloaded problem, $\theta = \omega/\omega_1$ respectively. The critical load $\hat{p}_{cr}$ for the Leipholz column is given in reference [7]. The non-dimensional load $\hat{p}$ for the column with an end load is defined as $\hat{p} = pL^2/EI$ and the associated critical load is given in reference [9].

### 4.1. SIMPLY–SIMPLY SUPPORTED BOUNDARY CONDITIONS

In this case, $a = 2$, $\lambda_n = n\pi$, and $\varphi_n(x) = \sin\lambda_n x$. Hence,

$$\mathbf{B} = \begin{bmatrix} -\pi^2/4 & -32/9 & 0 & -256/225 \\ -8/9 & -\pi^2 & -216/25 & 0 \\ 0 & -96/25 & -9\pi^2/4 & -768/49 \\ -16/225 & 0 & -432/49 & -4\pi^2 \end{bmatrix}. \tag{13}$$

Figure 3 shows the stability diagrams where the parametric planes are demarcated into stable and unstable regions as a function of excitation frequency

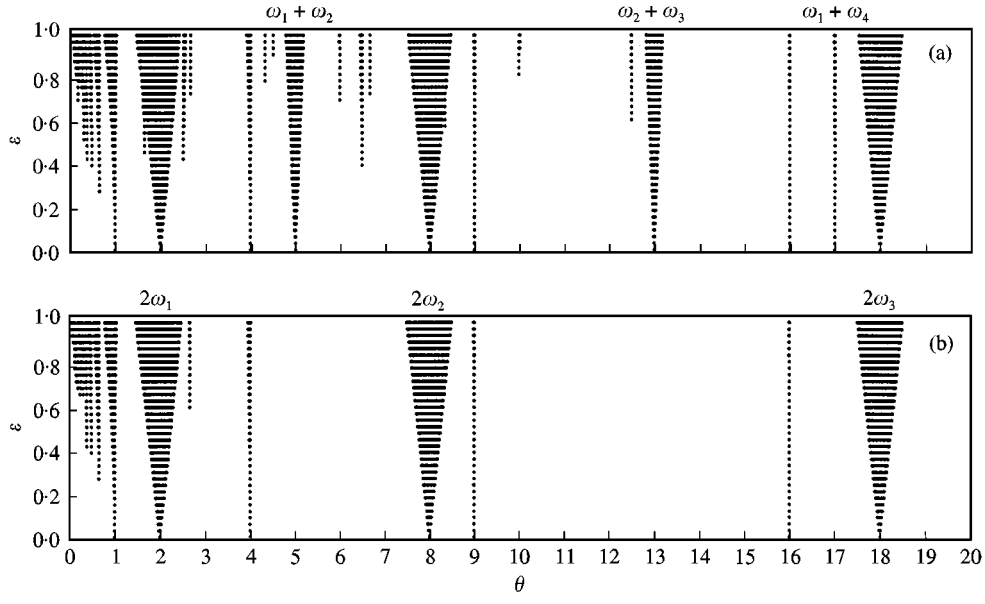


Figure 3. Stability diagram for a simply–simply supported column under (a) a distributed axial periodic load, (b) a periodic end load. Shaded areas are unstable regions.

$\theta$ and the excitation amplitude $\varepsilon$ with $\hat{p}_0 = 0$. Shaded areas denote unstable regions. Figure 3(a) shows the results for the Leipholz column and Figure 3(b) for a column excited by a periodic end load with the same excitation frequency. It is observed that the general behaviour of the two different systems is similar for the simple parametric resonance occurring at $\theta = 2, 8, 18$, and so on. However, the Leipholz column displays additional notable unstable regions at $\theta = 5, 13$, and 17 in the given range of frequencies. As shown in Figure 3(a), these unstable regions are readily identified as the results of combination resonance of sum type: viz., $\omega_1 + \omega_2, \omega_2 + \omega_3$, and $\omega_1 + \omega_4$ respectively. These regions can be generalized as $\omega_m + \omega_{m+2n-1}$, where $m, n = 1, 2, 3, \ldots$. Since the natural frequencies of the S–S beam are $n^2\pi^2, n = 1, 2, 3, \ldots$, one may argue that the instability regions at $\theta = 5, 13, 17$ are due to combination resonance of difference type; viz., $\omega_3 - \omega_2, \omega_7 - \omega_6$, and $\omega_9 - \omega_8$, respectively, instead of the sum type. However, based on the criterion for small $\varepsilon$ given by Hsu [11], it is stated that the condition for the existence of combination resonance of difference type is

$$|\theta - (\omega_n - \omega_m)| < \frac{a\hat{p}_{cr}\varepsilon}{2}\sqrt{-\frac{b_{mn}b_{nm}}{\omega_m\omega_n}} \quad (m < n). \tag{14}$$

For this problem, condition (14) cannot be satisfied with $b_{mn} > 0, \forall m, n$ given by equation (13). Therefore, combination resonance of the sum type exists for the Leipholz column with simply supported boundary conditions, but not the difference type. Note that a column with the same boundary conditions and excited

by a periodic end load does not have any combination resonance as shown in Figure 3(b).

### 4.2. CLAMPED–CLAMPED BOUNDARY CONDITION

In this case, $a = 1$, $\lambda_n = \{4{\cdot}73004, 7{\cdot}85321, 10{\cdot}99561, 14{\cdot}13717, \ldots\}$, and

$$\varphi_n(x) = \cosh \lambda_n x - \cos \lambda_n x - \frac{\cosh \lambda_n - \cos \lambda_n}{\sinh \lambda_n - \sin \lambda_n}(\sinh \lambda_n x - \sin \lambda_n x). \tag{15}$$

Hence,

$$\mathbf{B} = \begin{bmatrix} -6{\cdot}151 & -6{\cdot}685 & 4{\cdot}865 & 1{\cdot}537 \\ -0{\cdot}006 & -23{\cdot}025 & -15{\cdot}660 & 8{\cdot}564 \\ 4{\cdot}865 & -4{\cdot}628 & -49{\cdot}452 & -28{\cdot}529 \\ 3{\cdot}350 & 8{\cdot}564 & -13{\cdot}264 & -85{\cdot}793 \end{bmatrix}. \tag{16}$$

The corresponding stability diagram for this system is shown in Figure 4(a). Similar results can be observed as in the previous case regarding the additional unstable regions shown in Figure 4(a). In this case, combination resonance, of the sum type between any two different modes exists for the Leipholz column since $b_{mn} \neq 0$ for any $m$ and $n$. Note that the column with the same boundary conditions and excited by a periodic end load exhibits combination resonance of the sum type

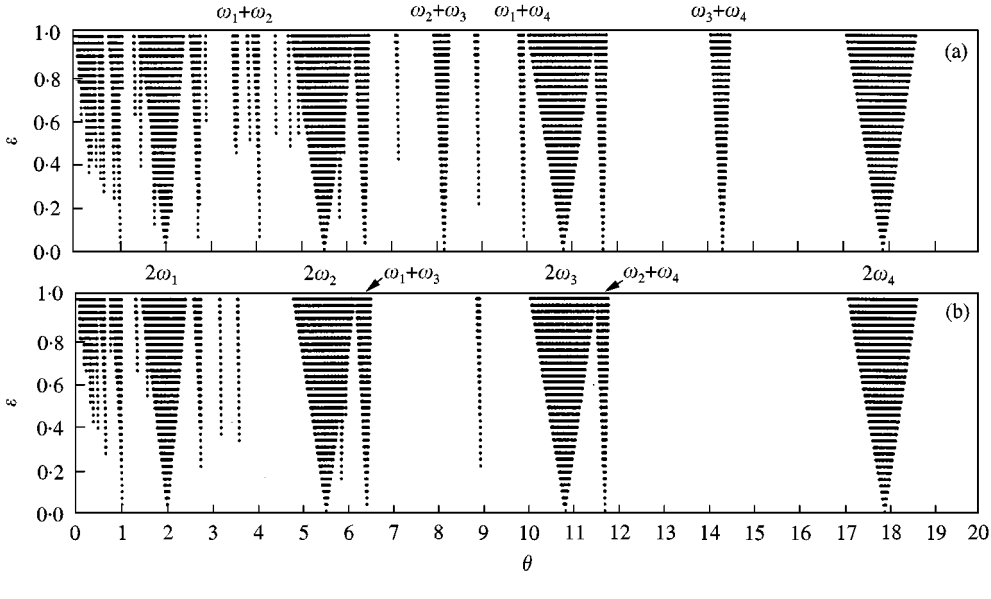


Figure 4. Stability diagram for a clamped–clamped column under (a) a distributed axial periodic load, (b) a periodic end load. Shaded areas are unstable regions.

only between $m$th and $(m + 2n)$th modes $(m, n = 1, 2, 3, \ldots)$ as shown in Figure 4(b). No combination resonance of a difference type exists for either column model since $b_{mn}b_{nm} > 0$ as in the S–S case.

### 4.3. CLAMPED–SIMPLY SUPPORTED BOUNDARY CONDITION

In this case, $a = 2$, $\lambda_n = \{3{\cdot}92660, 7{\cdot}06859, 10{\cdot}21018, 13{\cdot}35177, \ldots\}$, and

$$\varphi_n(x) = \sin \lambda_n x - \frac{\sin \lambda_n}{\sinh \lambda_n} \sinh \lambda_n x. \tag{17}$$

Hence,

$$\mathbf{B} = \begin{bmatrix} -3{\cdot}608 & -4{\cdot}675 & -0{\cdot}142 & -1{\cdot}247 \\ -1{\cdot}680 & -12{\cdot}241 & -10{\cdot}324 & -0{\cdot}011 \\ 0{\cdot}175 & -5{\cdot}177 & -25{\cdot}812 & -17{\cdot}897 \\ -0{\cdot}239 & 0{\cdot}243 & -10{\cdot}659 & -44{\cdot}317 \end{bmatrix}. \tag{18}$$

Note that $b_{13}b_{31} < 0$, $b_{24}b_{42} < 0$, or in general

$$\begin{aligned} &b_{m\{2(m+n)-1\}}b_{\{2(m+n)-1\}m} < 0 \quad \text{for odd } m \text{ and } n = 1, 2, 3, \ldots, \\ &b_{m\{2(m+n)\}}b_{\{2(m+n)\}m} < 0 \quad \text{for even } m > 0 \text{ and } n = 0, 1, 2, \ldots. \end{aligned} \tag{19}$$

This indicates that there exists a combination resonance of the difference type between two modes satisfying the relationships given by equation (19). However, as shown in Figure 5, these unstable regions are narrow and the amplitude growth rates in these regions are negligibly small, about order of $10^{-5}$, under $\varepsilon$ is large. It is also seen that the unstable regions for the Leipholz column are wider than the column with a periodic end load. In particular, the widths of the unstable regions of $\omega_2 + \omega_3$ and $\omega_3 + \omega_4$ are significantly different between the two column models.

### 4.4. CLAMPED–FREE BOUNDARY CONDITION

In this case, $a = 1$, $\lambda_n = \{1{\cdot}87511, 4{\cdot}69409, 7{\cdot}85476, 10{\cdot}9955, \ldots\}$, and

$$\varphi_n(x) = \cosh \lambda_n x - \cos \lambda_n x - \frac{\cosh \lambda_n + \cos \lambda_n}{\sinh \lambda_n + \sin \lambda_n} (\sinh \lambda_n x - \sin \lambda_n x). \tag{20}$$

Hence,

$$\mathbf{B} = \begin{bmatrix} 0{\cdot}429 & -4{\cdot}337 & 4{\cdot}856 & -3{\cdot}247 \\ 1{\cdot}182 & -6{\cdot}647 & -8{\cdot}112 & 7{\cdot}027 \\ 1{\cdot}288 & 0{\cdot}332 & -22{\cdot}952 & -16{\cdot}507 \\ 0{\cdot}993 & 4{\cdot}260 & -4{\cdot}170 & -49{\cdot}459 \end{bmatrix}. \tag{21}$$

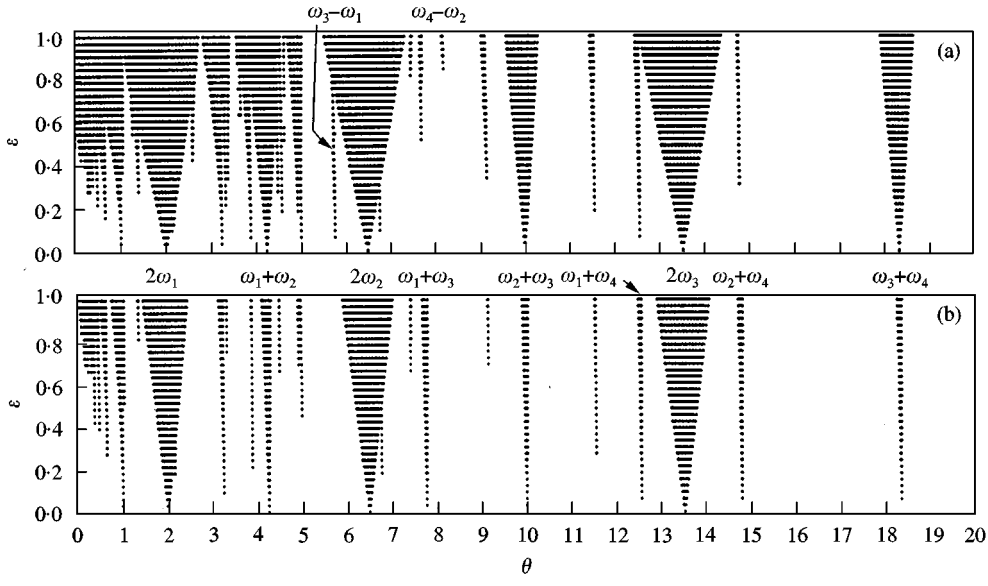


Figure 5. Stability diagram for a clamped–simply supported column under (a) a distributed axial periodic load, (b) a periodic end load. Shaded areas are unstable regions.

Note that $b_{12}b_{21} < 0$, $b_{14}b_{41} < 0$, and $b_{23}b_{32} < 0$. Therefore there exists a combination resonance of the difference type as in the previous case. However, for this case, it is difficult to observe a general pattern of the combination resonance between any two modes even by increasing the size of **B**. The following list gives the first nine pairs of modes for which combination resonances of the difference type occur: (1, 2), (1, 4), (1, 7), (1, 9), (2, 3), (2, 5), (2, 6), (2, 8), and (2, 10). For the clamped–free column excited by a periodic end load, combination resonances of the difference type occurs between the $m$th and $(m + 2n - 1)$th modes $(m, n = 1, 2, 3, \ldots)$ [9]. Figure 6 shows the corresponding stability diagram for each column model. It is seen that the unstable regions for both columns are much wider than in the previous cases due to the absence of the geometric constraint at the free end. It is observed that unstable regions for the column with a periodic end load are wider than those for the Leipholz column.

Note that the stability diagrams do not reveal the amplitude growth rate of the steady state response. This information is obtained by plotting $s_{real}$ against the $\theta$–$\varepsilon$ plane for the unstable regions. Figure 7 shows the results for the C–F case. It is observed that, for both columns, the growth rates and the widths in the region of $\omega_2 - \omega_1$ are almost as large as those in the region of $2\omega_2$ and are much larger than those in the unstable region of $2\omega_1$. These results indicate that a combination resonance of the difference type is just as important as the simple parametric resonance.

Note that the above results are for $\hat{p}_0 = 0$. When $\hat{p}_0 \neq 0$, the natural frequencies $\tilde{\omega}_j$ of the Leipholz C–F column are obtained by solving the eigenvalue problem (7) with $\hat{p} = 0$. Figure 8 shows the loci of $\tilde{\omega}$ as a function of the normalized follower load ($\varepsilon_0 = \hat{p}_0/\hat{p}_{cr}$; $\hat{p}_{cr} = 40{\cdot}7$ for the Leipholz column [7], $\hat{p}_{cr} = 20{\cdot}05$ for Beck's

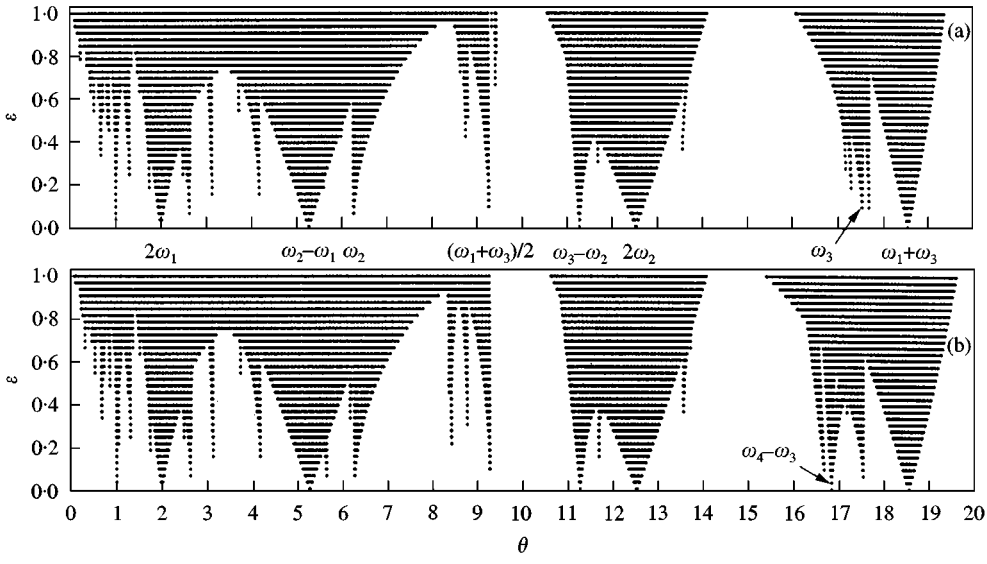


Figure 6. Stability diagram for a clamped–free column under (a) a distributed axial periodic load, (b) a periodic end load. Shaded areas are unstable regions.

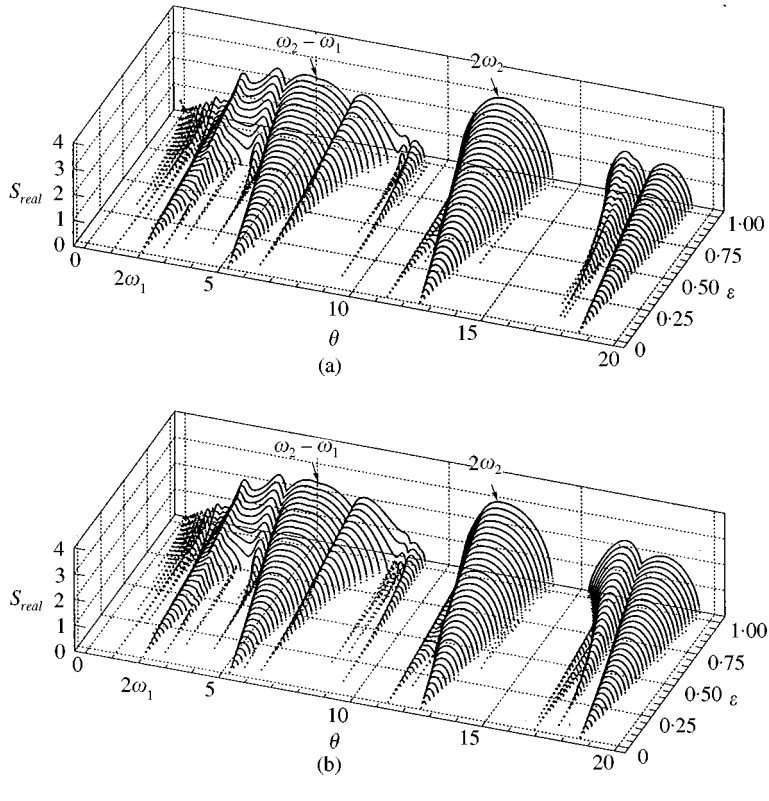


Figure 7. The amplitude growth rate of the unstable frequency response for a clamped–free column under (a) a distributed axial periodic load, (b) a periodic end load.

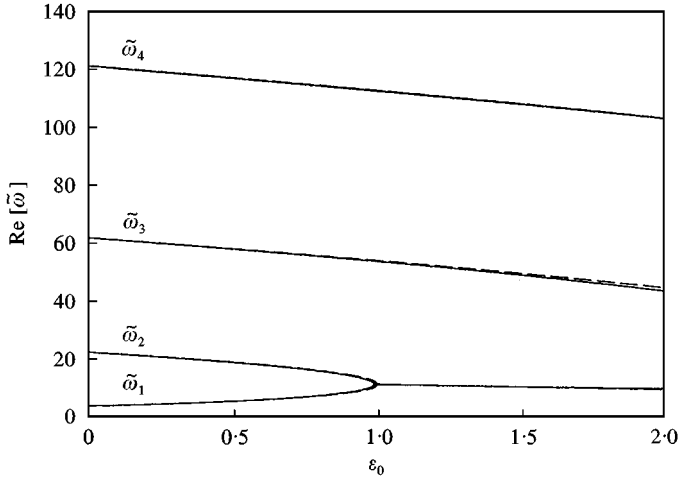


Figure 8. Loci of natural frequencies for a clamped-free column under a distributed follower-type axial load (——) and a follower-type end load (– – –).

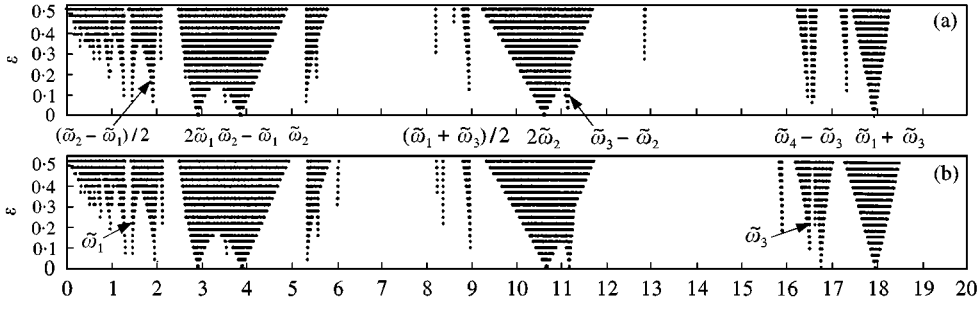


Figure 9. Stability diagram for a clamped-free column under (a) a distributed axial periodic load, (b) a periodic end load when $\hat{p}_0 = 0{\cdot}48\hat{p}_{cr}$. Shaded areas are unstable regions.

column [1, 9]). As expected, $\tilde{\omega}_1$ and $\tilde{\omega}_2$ coalesce at $\varepsilon_0 = 1$, leading to a flutter instability. It is noted from Figure 8 that both columns show almost the same qualitative relationships between $\tilde{\omega}_j$ and $\varepsilon_0$. Figure 9 plots the regions of parametric instability for $\hat{p}_0 = 0{\cdot}48\hat{p}_{cr}$. Comparing Figures 6 and 9, it is seen that the major effect of $\hat{p}_0$ is to shift the instability regions along the $\theta$-axis. This shift can be predicted based on Figure 8. For example, the $2\tilde{\omega}_1$ and $2\tilde{\omega}_2$ regions are shifted to the right and left of the frequency spectrum, respectively, while the $\tilde{\omega}_3 - \tilde{\omega}_2$ region is not shifted much. Moreover, as $\varepsilon_0$ increases ($\varepsilon_0 < 1$), $\tilde{\omega}_2 - \tilde{\omega}_1$ decreases and $2\tilde{\omega}_1$ increases such that $\tilde{\omega}_2 - \tilde{\omega}_1$ may become smaller than $2\tilde{\omega}_1$, as shown in Figure 10 for $\varepsilon_0 = 0{\cdot}81$. Thus, a combination resonance of the difference type may occur at a frequency lower than that of the principal parametric resonance of $2\tilde{\omega}_1$.

## 5. SUMMARY AND CONCLUSIONS

The parametric instability of a Leipholz column subjected to a periodic load is examined for four sets of boundary conditions. This prototypical model is believed

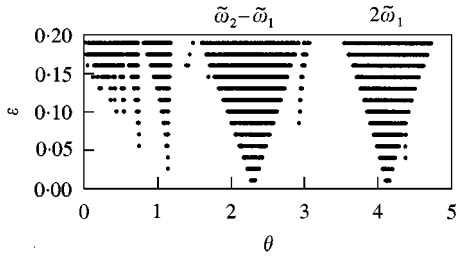


Figure 10. Stability diagram for the clamped–free Leipholz column when $\hat{p}_0 = 0{\cdot}81\hat{p}_{cr}$. Shaded areas are unstable regions.

TABLE 1

*Summary of the parametric instability characteristics for a column with different sets of boundary conditions*

| Boundary conditions | Combination resonance type | Distributed load (Leipholz column) | Concentrated end load[†] |
|---|---|---|---|
| Simple–simple | Difference | None | None |
| | Sum | $(m, m + 2n - 1)$[‡] | None |
| Clamped–clamped | Difference | None | None |
| | Sum | $(m, n)$ | $(m, m + 2n)$ |
| Clamped–clamped | Difference | $(m, 2(m + n) - 1)$ for odd $m$<br>$(m, 2(m + n))$ for even $m$[§] | None |
| | Sum | Other pairs of modes | $(m, n)$ |
| Clamped–free | Difference | (1, 2), (1, 4), (2, 3),[¶] … | $(m, m + 2n - 1)$ |
| | Sum | Other pairs of modes | Other pairs of modes |

[†]Iwatsubo *et al.* [9].

[‡]Denotes combination resonance of sum type between the $m$th and $(m + 2n - 1)$th modes, where $m, n = 1, 2, 3, \ldots$.

[§]For this case only, $n = 0, 1, 2, \ldots$.

[¶]No simple general pattern is observed (see section 4.4).

to reveal the fundamental instability characteristics of a disc brake pad under follower-type friction load. It is found that the boundary conditions strongly determine the types of combination resonance. Moreover, the combination resonance is shown to be as important as the simple parametric resonance. Results are compared to those for a column excited by a periodic end load under the same boundary conditions. It is found that the parametric instability of these two columns are considerably different and hence the effects of the distributed load must be carefully considered in the model. For the Leipholz column, a combination resonance of the sum type exists for all the boundary conditions considered in this study. However, this is not true for the column under a periodic end load. Moreover, the combination resonance of the difference type is found to be significant only in the clamped–free case for both columns. The occurrences of the various types of combination resonances is summarized in Table 1. It is also shown

that the constant follower load basically shifts the instability regions along the frequency axis. As this load increases, the combination resonance of the difference type may occur at a frequency lower than that of the principal parametric resonance.

This study shows that the instability of a brake pad depends strongly on the braking pressure and the friction material (these effects are embedded in the parameter $\varepsilon$), the design of the brake pad (through the boundary conditions), and the design of the brake disc ($\omega$ is related to the disc mode number). To avoid brake pad resonance, the disc rotor must be designed so that its natural frequencies are such that the associated modes would not excite the pad into resonance. Future work underway includes the study of the brake pad instability with a non-linear contact model.

## ACKNOWLEDGMENT

The authors acknowledge the support of Ford Motor Company University Research Grant for this research.

## REFERENCES

1. M. Beck 1952 *Zeitschrift für Angewandte Mathematik und Physik* (*ZAMP*) **3**, 255–228. Die Knicklast des einseitig eingespannten, tangential gedrückten Stabes.
2. V. V. Bolotin 1963 *Nonconservative Problems of the Theory of Elastic Stability*. New York: Pergamon Press, distributed by the MacMillan Company.
3. V. V. Bolotin 1964 *Dynamic Stability of Elastic Systems*. San Francisco: Holden-Day.
4. H. Ziegler 1968 *Principles of Structural Stability*. New York: Blaisdell Publishing.
5. H. H. E. Leipholz 1977 *Direct Variational Methods and Eigenvalue Problems in Engineering*. Leyden: Noordhoff International Publishing.
6. G. J. Simitses 1976 *An Introduction to the Elastic Stability of Structures*. Englewood Cliffs, NJ, Prentice-Hall.
7. H. H. E. Leipholz 1972 *ASME Journal of Applied Mechanics* **39**, 717–722. On the sufficiency of the energy criterion for the stability of certain nonconservative systems of the follower-load type.
8. H. H. E. Leipholz 1986 *Computer Methods in Applied Mechanics and Engineering* **59**, 215–226. On principles of stationary for non-self-adjoint rod problems.
9. T. Iwatsubo, Y. Sugiyama and S. Ogino 1974 *Journal of Sound and Vibration* **33**, 211–221. Simple and combination resonances of columns under periodic axial loads.
10. A. H. Nayfeh and D. T. Mook 1979 *Nonlinear Oscillations*. New York: John Wiley & Sons.
11. C. S. Hsu 1963 *ASME Journal of Applied Mechanics* **30**, 367–372. On the parametric excitation of a dynamic system having multiple degrees of freedom.
12. L. O. Chua and A. Ushida 1981 *IEEE Transactions on Circuits and Systems* **28**, 953–971. Algorithm for computing almost periodic steady-state response of nonlinear systems to multiple input frequencies.
13. Y. B. Kim and S. T. Noah 1991 *ASME Journal of Applied Mechanics* **58**, 543–553. Stability and bifurcation analysis of oscillators with piecewise-linear characteristics: a general approach.
14. S. K. Lau and Y. K. Cheung 1981 *ASME Journal of Applied Mechanics* **48**, 959–964. Amplitude incremental variational principle for nonlinear vibration of elastic systems.

15. S. C. SINHA and D.-H. WU 1991 *Journal of Sound and Vibration* **151**, 91–117. An efficient computational scheme for the analysis of periodic systems.
16. C. A. TAN and B. KANG 1998 *Ford Motor Company Technical Report No. TAN/TR*-98-02. A study on the root causes of disc brake squeal.
17. A. FELSKE, G. HOPPE and H. MATTHAI 1978 *SAE Paper No.* 780333. Oscillations in squealing disk brakes—analysis of vibration modes by holographic inteferometry.
18. J. D. FIELDHOUSE and P. NEWCOMB 1993 *SAE Paper No.* 930805. The application of holographic interferometry to the study of disc brake noise.
19. J. HULTÉN 1993 *Proceedings of SAE Trunk and Bus Meeting, Detroit, MI, November, Paper No.* 932695. Brake squeal—a self-exciting mechanism with constant friction.
20. K. TAKAHASHI 1981 *Journal of Sound and Vibration* **78**, 519–529. An approach to investigate the instability of the multiple-degree-of-freedom parametric dynamic systems.
21. S. K. SINHA 1989 *Journal of Sound and Vibration* **131**, 509–514. Dynamic stability of a Timoshenko beam subjected to an oscillating axial force.
22. J. HULTÉN and J. FLINT 1999 *Proceedings of the SAE International Congress and Exposition, Detroit, MI, March, Paper No.* 1999-01-1335. An assumed modes method approach to disc brake squeal analysis.
23. A. L. RUINA 1985 *Mechanics of Geomaterials* (Z. BAZANT, editor), 169–188. New York: John Wiley & Sons. Constitutive relations for fractional slip, chapter 9.
24. R. A. IBRAHIM 1994 *ASME Applied Mechanics Reviews* **47**, 209–226. Friction-induced vibration, chatter, squeal, and chaos, Part I: mechanics of contact and friction.
25. J. W. RICHMOND, T. K. KAO and M. W. MOORE 1996 *Advances in Automotive Braking Technology* (D. C. BARTON, editor), 69–86. The development of computational analysis techniques for disc brake pad design.

## APPENDIX A: DERIVATION OF EQUATION OF MOTION

In this section, it is shown that the equation of motion governing the vibration of a disc brake pad under the excitation of a rotating disc is fundamentally the same as the prototypical Leipholz column model under periodic excitation. Experiments have shown that there is no nodal circle in the disc vibration during braking [17, 18]. This allows us to consider a strip of arbitrary width of the disc brake pad as shown in Figure 1(a). Neglecting the curvature, the strip may be modelled as a beam under a distributed normal load (due to brake pressure) moving at speed $v = R\Omega_1$, where $R$ is the radius corresponding to the strip and $\Omega_1$ is the spinning speed of the disc. The use of the beam-like model has been validated experimentally [22], where the brake disc is modelled by an Euler–Bernoulli beam and the pad as a foundation. The theory predicts an instability at seven nodal diameters (i.e., seven nodal points in the beam model) and is verified by experiments on a vehicle.

The relative sliding motion of the disc generates a distributed traction on the surface of the pad due to friction. Assuming plane stress, the surface traction is transformed onto the centroid of the beam as a distributed axial load $\mu p_c$ (see Figure A1), where $p_c$ is the contact pressure and $\mu$ is the coefficient of friction between the disc and pad. The interface tribology is complicated and other more complex friction models have been proposed [23, 24].

The following assumptions apply to the brake pad model: (1) the brake disc and pad lining are in a state of elastic conformal contact; (2) there is no loss of contact or lift-off at any point in the contact interface between the disc and pad lining; (3) the

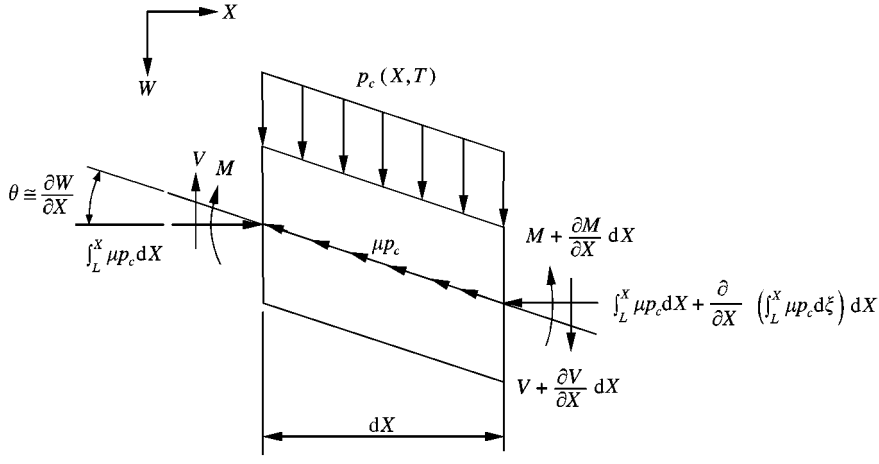


Figure A1. Free body diagram of a beam element subjected to distributed transverse and friction-induced axial load.

material properties of the pad and $\mu$ remain constant; (4) the variation of the normal contact load is caused by the vibration of the disc and fluctuates about the equilibrium state; and (5) other sub-structures such as the caliper piston, caliper and its mounting bracket are considered rigid.

Based on these assumptions, the instantaneous distributed contact normal load can be written as the sum of the static and dynamic normal loads,

$$p_c = p_0 + p(X, T). \tag{A1}$$

In general, $p(X, T)$ is a non-linear function of the relative transverse displacement between the disc and pad. Denote the transverse stiffness of the pad lining by $K$. Then $p_c$ may be expressed in terms of the transverse displacement as

$$p_c(X, T) = K(\Delta + \delta(X, T))^n = K(\Delta + W_r - W)^n, \tag{A2}$$

where $\Delta$ is the equilibrium deformation of the lining due to braking pressure, $W_r$ and $W$ are the transverse displacements of the rotor and pad respectively. The constants $K$ and $n$ can be determined experimentally [24, 25]. Since the displacement of a spinning disc mode in the circumferential direction is a harmonic function, $W_r$ may be represented as

$$W_r = f(\gamma X - \gamma R\Omega_1 T)g(\Omega_2 T), \tag{A3}$$

where $f(\cdot)$ is the travelling wave component in the circumferential direction with wavenumber $\gamma$ corresponding to the number of nodal diameters of the disc mode and $g(\cdot)$ is the excitation component as a function of the disc mode frequency $\Omega_2$.

We assume a sinusoidal form for $f(\cdot)$,

$$W_r = \alpha \sin(\gamma X - \gamma R\Omega_1 T)\cos(\Omega_2 T), \tag{A4}$$

where $\alpha$ denotes a constant amplitude of the vibrating disc mode.

Figure 1(b) depicts the beam model in a state of vibration and a free body diagram is shown in Figure A1. Neglecting the coupling between the transverse and axial vibrations and applying the Euler–Bernoulli beam theory, the linear equation of motion for the transverse displacement of the undamped beam under a moving distributed load is

$$\rho A \frac{\partial^2 W}{\partial T^2} + EI \frac{\partial^4 W}{\partial X^4} + \frac{\partial}{\partial X}\left(\mu \int_X^L \{p_0 + p(\xi, T)\}\, \mathrm{d}\xi \frac{\partial W}{\partial X}\right) + \mu p_c(X, T)\frac{\partial W}{\partial X}$$

$$+ K_p \sum_{i=1}^{2} \delta(X - L_i) W = p(X, T), \tag{A5}$$

which reduces to

$$\rho A \frac{\partial^2 W}{\partial T^2} + EI \frac{\partial^4 W}{\partial X^4} + \mu \int_X^L \{p_0 + p(\xi, T)\}\, \mathrm{d}\xi \frac{\partial^2 W}{\partial X^2} + K_p \sum_{i=1}^{2} \delta(X - L_i) W = p(X, T), \tag{A6}$$

where $\rho$ denotes the mass density of the beam, $A$ the cross-sectional area, $EI$ the flexural rigidity of the beam, $L$ the pad length, $K_p$ the (effective) elastic stiffness of the piston against the pad, and $L_i$ the locations of contact points between the piston and pad.

Note that for the outer pad where there is no piston in most automotive disc brake systems, $K_p = 0$. By equations (A2) and (A4) and enforcing $\Omega_2 \gg \Omega_1$ and $\Omega_1 \ll 1$ for typical disc brake applications, $p(\xi, T)$ is rewritten as $p(\xi)\cos\Omega_2 T$. The free vibration stability of the brake pad model (A6) thus reduces to equation (1) which is a Leipholz column under a periodic, deformation induced follower-type load.